LITHIUM ABUNDANCES IN F5–G8 DWARFS*

G. H. HERBIG
Lick Observatory, University of California
Received September 24, 1964

ABSTRACT

A survey of some 100 nearby F5–G8 dwarfs at 4 and 16 Å/mm with the coudé spectrograph, 120-inch telescope, has shown that there is a major variation in their lithium abundances, from values of $l \equiv (\mathrm{Li/Ca})^*/(\mathrm{Li/Ca})_\odot$ as large as 35 down to the limit of detection near $l \approx 1$. The fundamental hypothesis under test is whether these results can be explained by convective destruction of Li on a long time scale, following the arrival of each star on the main sequence with a Li content comparable with that found in the pre–main-sequence T Tauri stars. If there is no subsequent replacement of the Li, its abundance should decay exponentially with a time constant t_c, which is expected to be sharply mass-dependent Comparison of the present solar Li abundance with that of chondritic meteorites yields a value of $t_{c\odot} = 1\ 32 \times 10^9$ years. This time dependence can in principle be checked against the Li abundances of F–G dwarfs in galactic clusters of known age. Observations are available for seven stars in the Hyades, one in the Pleiades, and three in Coma. The abundances show a trend that conforms to expectation, but the scatter is not negligible, and the test cannot be considered a critical one.

Less direct checks are possible through correlations of Li abundances with other convection- and age-dependent properties. The frequency function of l varies with main-sequence spectral type (i.e., with mass) in the sense that in the F's, stars of all l values are present in roughly comparable numbers; while toward the later G's, large l values become rare, and after G8, no Li has been detected at all in K, M, or Me dwarfs. There is also a rather good correlation between low l values and high space velocities, and conversely. The correlation between (photometric) metal abundance and l is in qualitative accord with expectation in the G dwarfs, namely, that the Li-rich stars tend to have the higher metal abundances, but no such relationship is apparent in the later F stars. This difference may result from the shallower convection zones in the F stars, or a lack of a tight dependence of metal content upon age. There is also a statistical correlation between l and the strength of Ca II emission cores for G5 and earlier, as expected from evolutionary considerations based on the T Tauri stars, but individual objects show a considerable scatter.

In general, both components of spectroscopic and visual binary pairs show consistent Li abundances so long as they do not span the Li "cutoff" near K0, but ξ UMa constitutes an exception, which may however be explained by rotation-induced shortening of t_c in the fainter component. The relative rates of formation of F–G dwarfs in the past should be inferable from the l statistics, provided that the proper values of t_c are known If the solar t_c is used, the results definitely do not show the expected excess of very old F–G dwarfs. Any of several explanations are possible, including that of replenishment of surface Li But in general the fundamental hypothesis is supported by the material studied here, although there are some points that still require explanation.

I. INTRODUCTION

Recognition of the fact that the very young T Tauri stars, as a class, are abnormally rich in lithium with respect to ordinary dwarfs raises the question of what happens to this element after these objects evolve out of the T Tauri phase and reach the main sequence themselves. There would seem to be three ways in which stars of about 1 solar mass could reduce their initial surface Li abundances:

1. The Li could be destroyed as a result of the deep convection that is present during pre–main-sequence contraction. From the viewpoint of the theory, it appears that this convective zone does not extend deep enough to deplete surface Li seriously in the time available, although the calculations cannot as yet be regarded as final (Ezer and Cameron 1963; Hayashi and Nakano 1963; Weymann and Moore 1963; Böhm 1963). And from the observational point of view, the fact (demonstrated in this paper) that many F- and G-type main-sequence stars are observed to have rather high Li abundances shows that convective depletion of Li during contraction cannot have been complete in this mass range.

* *Contributions from the Lick Observatory*, No. 177.

2. A first-approximation study of mass loss by T Tauri stars has recently been made by Kuhi (1964). The instantaneous rates of mass ejection are, at least in principle, readily determinable. Kuhi finds that in his sample of six stars, dm/dt ranges between 0.3×10^{-7} and 6×10^{-7} solar masses/year, with an average of 4×10^{-8} $m_\odot$/yr. An integration of these rates over the contraction time of a T Tauri star involves certain assumptions as to the variation of dm/dt with position on the evolutionary track. Kuhi estimated this factor from the statistics of T Tauri stars and, in combination with Iben's theoretical tracks, found that a star of 1.0 $m_\odot$ may altogether eject as much as 0.4 $m_\odot$ during contraction. Clearly, if material in such quantities is lost during contraction, the validity of the theoretical tracks themselves is open to question. But the ejection of material even in these quantities—presumably from the surface layers—does not necessarily mean that the star will be peeled down to Li-free regions, because during the period of most active mass ejection the star is largely or entirely convective, and thus probably Li-homogeneous to a good approximation.

3. This paper examines the assumption that the predominant process of Li depletion in stars of about 1 $m_\odot$ is convective destruction on a long time scale after the star reaches the main sequence, an idea first proposed by Greenstein and Richardson (1951). The observational material bearing on this point is summarized in Section VI. The theory that will be required to interpret the observations from this point of view is as follows.

Let the relative abundances (by number) of Li atoms at any level in the outer convection zone be $L(t)$ at time t; it is assumed that the zone is rapidly and continuously mixed so that $L(t)$ does not depend on depth, and the rate of circulation does not enter explicitly at all. The Li atoms have a lifetime against (p, α) reactions at a depth q (where q is the usual dimensionless variable $m(r)/m_*$) of $\tau(q)$, and are being replenished at the surface at a rate $A(t)$ atoms sec^{-1}. Then

$$\frac{dL(t)}{dt} = -\frac{L(t)}{t_c} + A(t)C, \tag{1}$$

where, following Weymann and Moore,

$$\frac{1}{t_c} \equiv \left\langle \frac{1}{\tau(q)} \right\rangle = \frac{\int dq/\tau(q)}{\int dq}, \tag{2}$$

the integrals being taken over the convection zone, and

$$C = \frac{\mu m_0}{(1 - q_f)\, m_*} \tag{3}$$

where μm_0 is the mean molecular weight in grams in the zone, and the denominator is the total mass of the zone; $1/C$ is the total number of atoms in the zone. Equation (1) has the solution

$$\frac{L(t)}{L(0)} = e^{-t/t_c} + \frac{C}{L(0)}\, e^{-t/t_c} \int_0^t A(t)\, e^{t/t_c}\, dt, \tag{4}$$

where $L(0)$ is the relative Li abundance at $t = 0$. The term $A(t)$ has been retained to represent the possibility of Li replenishment by surface nucleosynthesis, an activity which one would expect to decay with t, perhaps on the same time scale as the chromospheric activity represented by the Ca II emission cores (see Sec. V). But for the present purpose, if $A(t)$ is set equal to A, equation (4) reduces to

$$\frac{L(t)}{L(0)} = e^{-t/t_c} + \frac{ACt_c}{L(0)} \left(1 - e^{-t/t_c}\right), \tag{5}$$

so that in the limit as $t \to \infty$, the Li abundance goes to a steady level of

$$L(t \to \infty) \to ACt_c\,. \tag{6}$$

But if Li replenishment is negligible from whatever source, the abundance simply decays exponentially

$$L(t) = L(0)\ e^{-t/t_c} \tag{7}$$

which is the expression to be used here.

In Table 1 are summarized the abundances (by number, on a scale of Si = 10^6) of Li, Be, and B in the solar atmosphere and in chondritic meteorites. If the meteoritic data collected by Shima and Honda (1963) are taken for the Li abundance of the solar surface at the time planetary material became separated from the Sun, then Mutschlecner's (1963) solar Li abundance indicates that in 4.7×10^9 years the Li (=$Li^7 + Li^7$) abundance has been reduced by a factor of about 35, which leads to a value of t_c in equation (7) of 1.32×10^9 years. One aim of this investigation is to determine whether the data for stars like the Sun are compatible with this value.

TABLE 1

ABUNDANCES OF THE LIGHT ELEMENTS

(Si = 10^6 atoms)

	STONE METEORITES		SUN	
	Suess and Urey (1958)	Shima and Honda (1963)	Goldberg, Müller, and Aller (1960)	Mutschlecner (1963)
Li	100	36 0	0 29	1 1
Be	20	1 0	7 2	6 9
B	24	7 7	...	

II. OBSERVATIONS AND ANALYSIS

Unfortunately, the only Li I line that is detectable on ordinary spectrograms of stars with temperatures like the Sun is the first member of the principal series, at 6707 Å, and all that follows is based on observations of that single feature. The expected equivalent widths of both the next member of the series (at 3232 Å) and the strongest subordinate line (at 6103 Å) are near or below the limit of detectability, even for Li-rich G dwarfs, on the 120-inch coudé material obtained thus far, although both lines may be marginally present in a few favorable cases. Certainly the identification of the feature at 6707 Å with Li I is beyond reasonable doubt on the basis of wavelength agreement and structure (except when it is weak in the later-type stars). But some effort directed to the detection of these weaker Li I lines would be justified, in order to clinch the matter.

The observing program for the 6707-Å region was confined to main-sequence stars between F5 and G8, for the following reasons. (1) Stars of luminosity class IV and brighter were excluded because of their more complicated evolutionary history. (2) Types earlier than F5 were excluded because of the difficulty of finding very many sharp-lined stars that were not peculiar in some way, and because of the very high degree of Li ionization at those temperatures. Many F5–F8 stars were not observed because they were known to have excessive rotational line broadening. (3) Types of K0 and later were

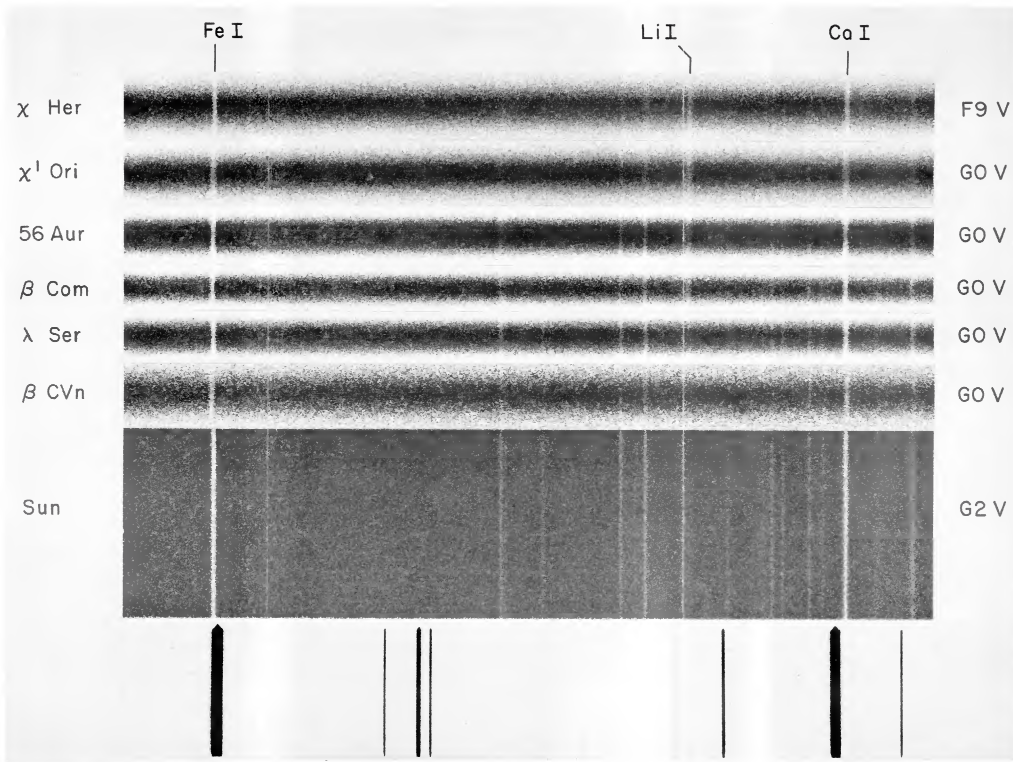

FIG. 1.—Representative 4-Å/mm spectrograms of seven F9–G2 dwarfs in the 6670–6725 Å region, showing the range of Li I λ 6707 strengths observed among the nearby stars. The stronger feature near λ 6707 in the Sun is not due to Li I, but is the unidentified line at λ 6707.45. (Coudé spectrograph, 120-inch reflector, 160-inch camera.)

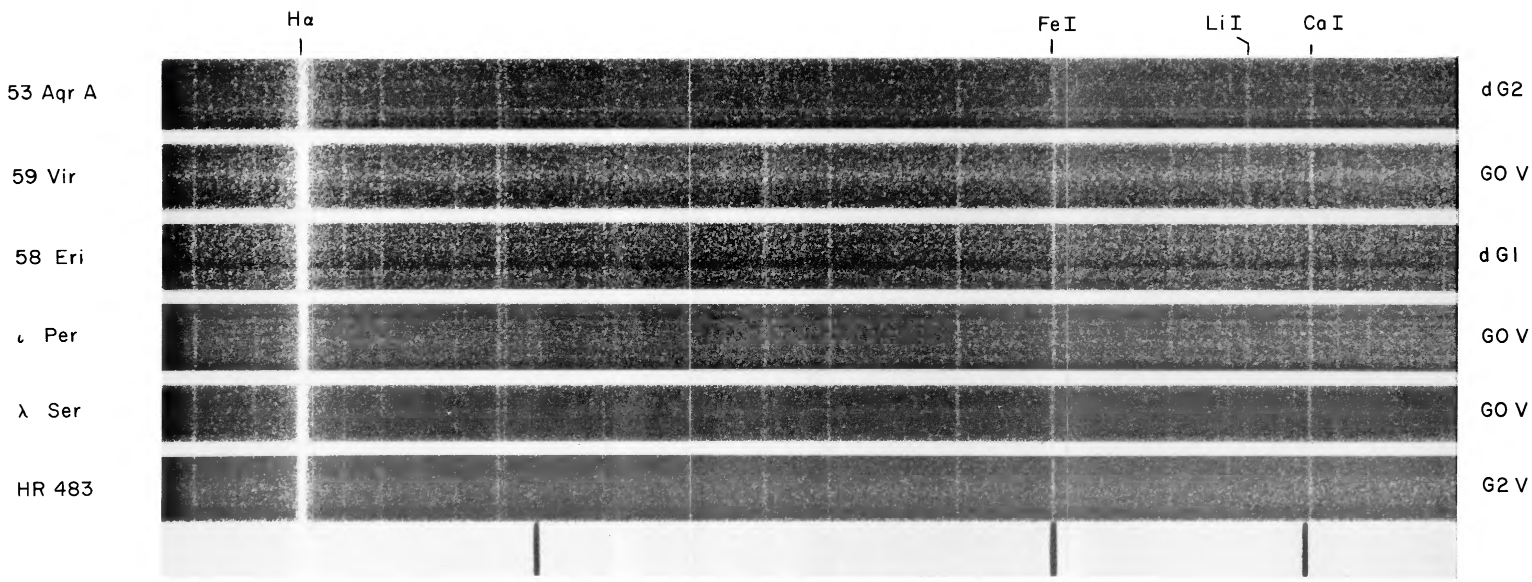

FIG. 2.—Spectrograms of nearby G0–G2 dwarfs at 16 Å/mm in the 6540–6750 Å region, showing the spread in Li I λ 6707 strengths, ranging from the strongest yet observed in normal stars (*top*) to invisibility (*bottom*). (Coudé spectrograph, 120-inch reflector, 20-inch camera.)

excluded because a representative sampling of K stars at 32-Å/mm dispersion and of M and Me dwarfs at 15 and 20 Å/mm showed none having λ 6707 certainly present. The same result had also been found by Bonsack (1959), and has since been confirmed by Wilson (1963*a*) on the basis of a larger sample of K stars. Such a result is to be expected on account of the very deep surface-convection zones of late-type dwarfs, as was pointed out by Bonsack, but this is not the only possible explanation. For instance, Hayashi and Nakano (1963) have demonstrated that in stars of 0.6 $\mathfrak{m}_\odot$ and less, major Li depletion is possible during pre–main-sequence contraction.

Observations for Li abundance have also been made of a sample of F-, G-, and K-type subgiants and of a large number of M giants, but those results will not be given here.

The observations were confined, except for a few stars of special interest, to stars within 20 parsecs in order to avoid undue statistical bias. The other restriction on the material is set by the declination limits of the 120-inch coudé spectrograph: +51°, the northern limit of the 3-mirror system, and about −25°, in order to avoid unduly long exposures. The observations were begun in 1961 at 4 Å/mm, but the exposure times were long and data accumulated very slowly. About a year later, the work was therefore shifted to 16 Å/mm, and only brighter stars of particular interest (or those suitable for investigation of the Li isotope ratio: see Herbig 1964*a*) were subsequently observed also at the higher dispersion. The 16-Å/mm spectrograms were obtained with the 20-inch camera, in the second order of a 600-groove/mm Babcock grating, and widened to 0.5 mm on Kodak 103*a*-F plates. The 4-Å/mm plates were exposed in the 160-inch camera, in the first order of another Babcock 600-groove/mm grating, and widened to 1–1.5 mm on Kodak 103*a*-F + 103*a*-D emulsions. Representative spectra at each dispersion are shown in Figures 1 and 2. The stars observed are listed in Table 2.

The plates were photometrically calibrated in the spectrograph, as the stellar exposure was being made, by a stepped-slit device and were traced in the Lick direct-intensity microphotometer. The equivalent widths of the smoothed profiles drawn through the photographic noise were obtained through a five-point integration formula. The curve-of-growth procedure for the 4-Å/mm plates was the standard differential comparison with the Sun; the detailed derivations will not be given here since they are available, for example, in Aller and Greenstein (1960) or in Aller (1963). Three solar spectrograms (of the daylight sky and the moon) were used to obtain log $W_\odot/\lambda$'s for some 100 relatively unblended Fe I, Fe II, and Ca I lines between 5110 and 6710 A. The empirical solar curve of growth of Goldberg and Pierce (Aller 1953) was entered with these log $W_\odot/\lambda$'s, and log $\eta_c{}_\odot$'s read off. The stellar log W^*/λ's for the Fe I lines were then plotted against their log $\eta_c{}_\odot$ values, and the empirical solar curve fitted to these points by eye inspection. This curve was then entered with the Fe I log W^*/λ values and preliminary log $\eta_c{}^*$'s read out. The difference between these and the solar values should be a linear function of ϵ, the lower excitation potential, with slope $\Delta\theta = \theta_{\rm exc}{}^* - \theta_{\rm exc}{}_\odot$. A least-squares solution was made for $\Delta\theta$, the curve replotted with $\log \eta_c{}^* = \log \eta_c{}_\odot - \epsilon\cdot\Delta\theta$ as abscissa, and the procedure repeated until no further improvement of $\Delta\theta$ was possible. The final Fe I curve was then slid horizontally and vertically by amounts $\Delta \log \eta_c{}^*$ and $\Delta \log W^*/\lambda$ into coincidence with the empirical solar curve, whose shifts to fit Wrubel's (1949) theoretical Milne-Eddington curve for $B^{(0)}/B^{(1)} = \frac{2}{3}$ are $\Delta \log \eta_c{}_\odot = -0.41$, $\Delta \log W_\odot/\lambda = +5.04$. It was assumed that $\Delta\theta$ is also equal to $\theta_{\rm ion}{}^* - \theta_{\rm ion}{}_\odot$, and that $\theta_{\rm exc}{}_\odot = 1.04$, $\theta_{\rm ion}{}_\odot = 0.89$, $\log P_e{}_\odot = +1.3$, which are appropriate values for an optical depth of $\tau_{\lambda 5500} = 0.35$ in the solar atmosphere.

Next, the log W^*/λ values for about twelve unblended Fe II lines were used to read log $\eta_c{}^*$'s from the Fe I curve of growth, and the mean of the quantities $r(\text{Fe II}) = (\log \eta_c{}^* + \epsilon\cdot\Delta\theta) - \log \eta_c{}_\odot$ for each Fe II line obtained. Now

$$\log \frac{N^*(\text{Fe II})}{N^*(\text{Fe I})} = \log \frac{N_\odot(\text{Fe II})}{N_\odot(\text{Fe I})} + \langle r(\text{Fe II})\rangle - \log\left(\frac{u^*}{u_\odot}\right)_{\text{Fe I}} + \log\left(\frac{u^*}{u_\odot}\right)_{\text{Fe II}}, \quad (8)$$

TABLE 2

FIELD STARS OBSERVED FOR LITHIUM ABUNDANCE

STAR (1)	HD (2)	α (1900) (3)	δ (3)	SP. TYPE (4)	4-Å/MM DETERMINATIONS [Li/Ca] (5)	[Fe/H] (6)	Δθ (7)	[v_{Fe}] (8)	[P_e] (9)	n (10)	16-Å/MM DETERMINATIONS [Li/Ca] (11)	n (12)	VIS. ESTS. I_{6707} (13)	ADOPTED [Li/Ca] (14)	WT. (15)	CA II EM. INT. (16)	PHOTO-METRIC [Fe/H] (17)	NOTES (18)
Sun				G2 V							≤+0.36	1	0	≤+0.4	b	0		
6 Cet.	693	0h06m2	−16°01′	F6 V									5	+1.1	c			
9 Cet.	1835	0 17 7	−12 46	dG2							+1.16	1	7	+1.2	b	4		
HR 159	3443	0 32.2	−25 19	G5 V									0, 1	≤+0.6	c	0		VB
	4747	0 44.4	−23 46	dG7									0	≤+0.5	c			
φ² Cet.		0 45.1	−11 11	F8 V	+1.34	+0.03	−0.05	−0.02	+0.21	1			7	+1.35	a		S	
	9540	1 28.5	−24 41	dG8									0	≤+0.5	c	2		
υ And.	9826	1 30.9	+40 54	F8 V							+0.82	1	1	+0.7	b		+0.17	
HR 483.	10307	1 35.7	+42 07	G2 V							≤+0.16	1	0	≤+0.1	b	0	+ 08	
τ Cet.	10700	1 39 4	−16 28	G8 Vp	≤+0.22	− 13	+ 02	+ .16	− 03	1			1	≤+0.3	a	0	S	
109 Psc.	10697	1 39.5	+19 35	dG4							+0.48	1	0, 1	+0.4	b	0		
	11131	1 44.4	−11 11	dG1							+1.03	1	5, 6	+1.0	b	3		
δ Tri.	13974	2 10.9	+33 46	G0 V	+1.08	− 18	+ 01	− 03	− 19	1			5	+1.08	a	2	− 04	SB2, *
HR 683.	14412	2 14.5	−26 25	G5 V									3:	+0.9:	c	0		
κ For	14802	2 18.0	−24 16	dG1									5·	+1.1:	c	0		
θ Per	16895	2 37.4	+48 48	F7 V	+1.26:	+ 07:	− 03:	− .01:	− .07:	1			5	+1.2	b		+ 14	*
ι Per.	19373	3 01.8	+49 14	G0 V	+0.97	+ .26	− 02	+ .02	+ .02	2	+1.07	2	5·	+0.97	a	0	+ .19	
94 Cet.	19994	3 07 7	− 1 34	F8 V									0, 1	≤+0.6	c		+ .23	
	20619	3 14.0	− 3 12	dG2									0:	≤+0.5·	c			
κ Cet.	20630	3 14.1	+ 3 00	G5 V	+0.83	+ .38	− .04	+ .12	+ 43	1	+0.93	1	3	+0.84	a	3	S	
10 Tau.	22484	3 31.8	+ 0 05	F8 V	+1.10	+ .37	− .04	− 03	+ .22	1	+1.30	1	4, 5	+1.12	a		S	*
39 Tau.	25680	3 59 4	+21 44	dG1							+0.94	1	4, 5	+0.9	b	3		
58 Eri.	30495	4 43.1	−17 07	dG1							+0.97	1	4	+0.9	b	5		
104 Tau.	32923	5 01.5	+18 31	G4 V									0	≤+0.5	c	0	− 4.	VB
68 Eri.	33256	5 03.8	− 4 35	F5 V									0	≤+0.5	c		− .22	
λ Aur.	34411	5 12.1	+40 01	G0 V									0	≤+0.5	c	0	+ .12	
γ Lep A.	38393	5 40.3	−22 29	F6 V	+1.11	− .07	.00	.00	− 40	2			3, 4	+1.08	a		S	
γ Lep B.		5 40.3	−22 27	K2 V									0	≤+0.5	c			
χ¹ Ori.	39587	5 48.5	+20 15	G0 V	+1.22	+ .25	− .02	+ .05	+ 03	2			7	+1.26	a	4	+ .06	
HR 2067	39881	5 50.3	+13 56	dG0									<3	<+0.9	c	0		
HR 2208	42807	6 07 7	+10 40	G6 V									3	+0.9	c			
56 Aur.	48682	6 39.5	+43 41	G0 V	+1.04	+0.15	−0 01	0.00	−0.04	1	+1.01	1	4, 5	+1.01	a		+ 19	
37 Gem.	50692	6 49.2	+25 30	dG0							≤+0.67	1	3	≤+0.7	b		−0.01	

TABLE 2—*Continued*

STAR (1)	HD (2)	α (1900) (3)	δ (3)	SP TYPE (4)	4-Å/MM DETERMINATIONS [Li/Ca] (5)	[Fe/H] (6)	Δθ (7)	[v_{Fe}] (8)	[P_e] (9)	n (10)	16-Å/MM DETERMINATIONS [Li/Ca] (11)	n (12)	VIS. ESTS. I_{6707} (13)	ADOPTED [Li/Ca] (14)	WT. (15)	Ca II EM. INT. (16)	PHOTOMETRIC [Fe/H] (17)	NOTES (18)
HR 2643	52711	6h57m2	+29°30′	dG2									0	≤+0.5	c		+0 18	
22 Lyn	58855	7 22.3	+49 53	F6 V									≤4.	≤+1.0:	c		− 07	
9 Pup	64096	7 47 1	−13 38	G1 V							+0.93	1	3, 4	+0.9	b	0		VB
	65583	7 54.3	+29 31	G8 V									<3	<+0.9	c			
18 Pup	68146	8 06.0	−13 30	dF7									4, 5:	+1.1.	c			
HR 3259	69830	8 13 6	−12 18	G8 V									0, 1	≤+0.6	c			
HR 3430	73752A	8 34.8	−22 19	dG6									0	≤+0.5	c			
HR 3538	76151	8 49 4	− 5 04	dG3									1	+0.6	c		+ 13:	
HR 3750	81809	9 22.8	− 5 38	G2 V							≤+0.1	1	0	≤+0.1	b		− 6:	VB
11 LMi	82885	9 29 7	+36 16	G8 IV–V									0	≤+0.5	c	1		
HR 3862	84117	9 37 7	−23 28	G0 V							+1.15	1	5	+1.1	b	0		
15 LMi	84737	9 42.1	+46 29	G3 V							+0.83	1	2	+0.8	b		+ 07	
20 LMi	86728	9 55.2	+32 25	G4 V									0, 1	≤+0.6	c	0	+ 06:	
HR 4098	90508	10 21.9	+49 19	G1 V									0	≤+0.5	c		− .23	
47 UMa	95128	10 53.9	+40 58	G0 V							≤+0.77	1	0	≤+0.7	b	0	+ 04	
HR 4345	97334	11 07 1	+36 21	sdG2							+1.37	1	6	+1.3	b		+ 12	
ξ UMa A	98231	11 12.8	+32 06	G0 V	+1.22	−0 01	−0 03	−0.06	+0 12	1			5	+1.20	a	≤1	S	SB1
ξ UMa B	98230	11 12.8	+32 06	G0 V	≤+0.39	− 12	+ 01	+ 08	− 10	1			1	≤+0.4	a	4	S	SB1
61 UMa	101501	11 35.8	+34 46	G8 V							≤+0.64	1	0	≤+0.5	b	2		
β Vir	102870	11 45.5	+ 2 20	F8 V									0	≤+0.5	c		+ .28	
	103095	11 47.2	+38 26	G8 VI							≤+0.40	1	0:	≤+0.3	b	2		*
HR 4587	104304	11 55.6	− 9 53	dG7									0	≤+0.5	c			
β CVn	109358	12 29 0	+41 54	G0 V	≤+0.50	+ 02	− 01	+ 03	− 08	1			0	≤+0.5	a	0	− 12	
10 CVn	110897	12 40.3	+39 49	G0 V							+1.03	1	2, 3	+0.9	b		− 40	
β Com	114710	13 07.2	+28 23	G0 V	+1.18	+ 08	− 02	+ 06	− 01	2	+1.24	1	5	+1.16	a	1	+ 14	
59 Vir	115383	13 11.8	+ 9 57	G0 V							+1.40	1	6	+1.3	b		+ 08	
61 Vir	115617	13 13.2	−17 45	G6 V									0	≤+0.5	c	0		
70 Vir	117176	13 23.5	+14 19	G5 V							+0.92	1	1	+0.8	b	1		
τ Boo	120136	13 42.5	+17 57	F7 V									2	+0.8	c			
HR 5273	122742	13 58.6	+11 16	G8 V							≤+0.43	1	0	≤+0.3	b			
HR 5384	126053	14 18.1	+ 1 43	dG3									2:	+0.8.	c		−0 13	
HR 5534	130948	14 45.8	+24 20	dG2							+1.44	1	6	+1.3	b			
ξ Boo A	131156	14 46.8	+19 31	G8 V	+1.35	0.00	+0 02	+0.20	+0 02	1	+1.52	1	6–7	+1.39	a	3	S	
ξ Boo B				dK5									<3					

TABLE 2—*Continued*

Star (1)	HD (2)	α (1900) (3)	δ (3)	Sp. Type (4)	4-Å/mm Determinations: [Li/Ca] (5)	[Fe/H] (6)	Δθ (7)	[v_{Fe}] (8)	[P_e] (9)	n (10)	16-Å/mm Determinations: [Li/Ca] (11)	n (12)	Vis. Ests. I_{6707} (13)	Adopted [Li/Ca] (14)	Wt. (15)	Ca II Em. Int. (16)	Photometric [Fe/H] (17)	Notes (18)
44 Boo.	133640	15h00m5	+48°03′	dG1									3, 4?	+1.0?	c			*
η CrB.	137107–8	15 19 1	+30 39	G2 V							+1.38:	1	4, 5?	+1.2	b			*
λ Ser	141004	15 41.6	+ 7 40	G0 V	≤+0.60	−0 04	0 00	+0 05	−0.10	1	+0.76	1	1	≤+0.6	a	0		
χ Her.	142373	15 49.2	+42 44	F9 V	+1.53	− 40	+ 02	+ 02	− 41	1			6	+1.48	a		−0 44	
ρ CrB.	143761	15 57.2	+33 36	G2 V									0	≤+0.5	c	0	− .23	
18 Sco.	146233	16 10.2	− 8 06	dG1									0, 1	≤+0.6	c			
	152391	16 48.0	+ 0 12	G6 V									0	≤+0.5	c	3		
	154345	16 59.8	+47 11	G8 V									0	≤+0.5	c	0		
72 Her.	157214	17 16.9	+32 36	G2 V							≤+0.48	1	0	≤+0.4	b	0	− .5·	
HR 6538.	159222	17 28.4	+34 21	G5 V							+1.01	1	3	+0.9	b	≤1		
99 Her A.	165908	18 03.2	+30 33	F7 V									5	+1.1	c		− .35	
HR 6998.	172051	18 32.9	−21 08	dG4									2?	+0.8?	c			
110 Her.	173667	18 41.4	+20 27	F6 V									0	≤+0.5	c		+ .01	
HR 7162A.	176051	18 53.3	+32 46	G0 V									1–2	+0.7	c	0		
HR 7260.	178428	19 03.5	+16 42	dG4									1	+0.6	c	0		SB1
HR 7451.	184960	19 31.7	+51 01	F8 V							+1.27	1	6–7	+1.2	b		− 06	
16 Cyg A.	186408	19 39.2	+50 18	G2 V									1	+0.6	c	0	− 1.	
16 Cyg B.	186427	19 39.2	+50 17	G5 V									0, 1	≤+0.6	c	0	− .1.	
17 Cyg A.	187013	19 42.6	+33 30	F5 V									3, 4?	+1.0?	c		+ 06	
ο Aql.	187691	19 46.2	+10 10	F8 V							+1.11	1	4	+1.0	b		+ .24	
15 Sge.	190406	19 59 6	+16 48	dG1									2	+0.8	c	1	+ .01	
27 Cyg.	191026	20 02.6	+35 42	dG3*									0	≤+0.5	c	4·		*
HR 7898.	196761	20 34.2	−24 08	dG7							≤+0.55	1	2?	≤+0.5	b	0		
HR 7914.	197076	20 36.2	+19 34	dG2							+1.02	1	4:	+0.9	b	0		
μ Cyg A.	206826	21 39 7	+28 17	F6 V									0	≤+0.5	c			
μ Cyg B.	206827			F8							≤+1.15	1	3, 4	≤+1.0	b			
ι Peg.	210027	22 02.4	+24 51	F5 V	+1.33	− .10	− 01	− 04	− .34	3			7	+1.34	a		+ 16	*
53 Aqr A.	212698	22 21.1	−17 15	dG2							+1.45	1	7	+1.4	b	5		
53 Aqr B.	212697			dG1							+1.61	1	7+	+1.5	b	4–5		
	214759	22 35.2	−32 30	G8 V							+0.34	1	<2	+0.2	b			
ξ Peg.	215648	22 41.7	+11 40	F7 V	+0.84	−0.05	0.00	+0.02	−0.34	1			4	+0.89	a		− 10	
51 Peg.	217014	22 52.6	+20 14	G5 V									0	≤+0.5	c	0	− 01:	
ι Psc.	222368	23 34.8	+ 5 05	F7 V							≤+0.44	1	0	≤+0.3	b		− 07	
85 Peg.	224930	23 57 0	+26 33	G3 V									0:	≤+0.5:	c	0	−0 7	

NOTES TO TABLE 2

Cols. (1)–(3) are self-explanatory.

Col (4) contains the MK type where available; all others (preceded by a *d*) are on the Mount Wilson system.

Cols (5)–(10) give the atmospheric parameters obtained from analysis of the 4-Å/mm spectrograms. The square brackets indicate logarithms of quantities in solar units; thus $[P_e] = \log P_e^*/P_e^{\odot}$. Col. (10) gives the number of plates upon which the foregoing results are based.

Cols. (11) and (12) give the results of the "shortcut" analyses, and the number of 16-Å/mm plates used

Col. (13) gives the visually estimated strengths of the Li I λ 6707 line, as described in Sec. II.

Col (14) gives the final mean value of [Li/Ca] resulting from a combination of all data, weighted as described at the end of Sec. II, and with the correction of Δ[Li/Ca] = −0.1 applied to the 16-Å/mm values.

Col. (15) gives the weight of this mean.

Col (16) contains the estimated strength of the Ca II emission cores, on the 0–5 scale of O C. Wilson. Values in italics are as published by Wilson; all others are new estimates on the same system.

Col (17) gives the *photometric* value of [Fe/H] as inferred from Strömgren's photometric Δm_1 index, as described in Sec. IV. For those stars for which narrow-band photometry was not available, the *spectroscopic* value of [Fe/H] has been used in the discussion; such stars have an *S* in col. (17).

Col. (18) employs the following abbreviations: VB = unresolved visual binary; SB1 = single-line spectroscopic binary; SB2 = double-line spectroscopic binary. An asterisk indicates the existence of a note for that star, as follows:

δ Tri: spectroscopic binary with $P = 9^{d}.9$. The spectrum of the secondary star appears on a 4-Å/mm plate of the yellow-red; Li I λ 6707 is present in both components.

θ Per: the plate is of poorer than average quality, and the results are of somewhat lower weight as a result.

10 Tau: according to Eggen (1963), this star is a subgiant.

HD 103095 = Groombridge 1830.

44 Boo: both components observed as one star.

η CrB: the result in the table refers to both components observed as one star. Subsequently, 16-Å/mm spectrograms were obtained of the individual stars; Li I λ 6707 is of similar strength in both components, but these plates have not been analyzed

27 Cyg: this star was included in the program because of the Wilson-Bappu (1957) classification as dG3. However, Miss Roman (1955) has classified it as K0 IV.

ι Peg: spectroscopic binary of $P = 10^{d}.2$. The secondary spectrum appears on the 4-Å/mm plates of the yellow-red Both components show Li I λ 6707.

where the u's are partition functions, for which Claas's (1951) tables were used, and the N's are expressed in atoms per gram of stellar material. The first term on the right is obtained from Saha's equation with the adopted values for the solar atmospheric parameters, so that

$$\log \frac{N^*(\mathrm{Fe\ II})}{N^*(\mathrm{Fe\ I})} = +0.91 + \langle r(\mathrm{Fe\ II}) \rangle - \log \frac{u^*(\mathrm{Fe\ I})}{u^*(\mathrm{Fe\ II})}. \tag{9}$$

Saha's equation also gives

$$\log P_e^* = +8.17 - \langle r(\mathrm{Fe\ II}) \rangle - 7.86\,\theta_{\mathrm{ion}}^* - 2.5 \log \theta_{\mathrm{ion}}^*, \tag{10}$$

and, if a negligible fraction of the Fe is doubly ionized,

$$\log \frac{N^*(\mathrm{Fe})}{N^{\odot}(\mathrm{Fe})} = -1.13 + \log \frac{N^*(\mathrm{Fe\ I})}{N^{\odot}(\mathrm{Fe\ I})} + \log\left[1 + \frac{N^*(\mathrm{Fe\ II})}{N^*(\mathrm{Fe\ I})}\right], \tag{11}$$

where the second term on the right comes from

$$\log \frac{N^*(\mathrm{Fe\ I})}{N^{\odot}(\mathrm{Fe\ I})} = \left(\Delta \log \eta_c^* - \Delta \log \eta_c^{\odot} - \Delta \log \frac{W^*}{\lambda} + \Delta \log \frac{W^{\odot}}{\lambda}\right) + \log \frac{\kappa^*}{\kappa^{\odot}} + \log \left(\frac{u^*}{u^{\odot}}\right)_{\mathrm{Fe\ I}} \tag{12a}$$

$$= +4.39 + \Delta \log \eta_c^* - \Delta \log W^*/\lambda + \log \kappa^*(\mathrm{Fe}) + \log u^*(\mathrm{Fe\ I}). \tag{12b}$$

Strictly, the continuous absorption coefficient κ(Fe) varies slowly from line to line, but the value for 6200 Å was employed throughout for all the Fe and Ca lines; the value at 6707 Å was used for the Li calculations. The numerical values of κ were interpolated as a function of $\theta_{\rm ion}$, log P_e, and λ in the convenient tables given by Allen (1963).

Once the atmospheric parameters have been obtained, the determination of

$$\frac{\rm Li}{\rm Ca} \equiv \log \frac{N({\rm Li})^*/N({\rm Ca})^*}{N({\rm Li})^\odot/N({\rm Ca})^\odot} \tag{13}$$

depends upon how one prefers to handle the fact that Li I λ 6707 is a blended doublet. Three possibilities are considered here, the first two following Bonsack (1959):

Case I.—assume that the two lines are intrinsically blended; i.e., that their absorption coefficients have to be added before the resultant profile is computed. Since one component has twice the strength of the other, we use for the Doppler width of the blend a value 1.5 times that of the stronger component.

TABLE 3

COMPARISON OF RESULTS WHEN REDUCTION TO [Li/Ca] WAS MADE ON ASSUMPTIONS OF CASES I, II, AND III

STAR	[Li/Ca] FOR		
	Case I	Case II	Case III
β Com	1 18	1 18	1 16
χ Her	1 53	1 55	1 53
γ Lep A	1 11	1 12	1 10
κ Cet	0 83	0 84	0 83
ϕ^2 Cet	1 34	1 34	1 32
δ Tri	1 08	1 10	1 07
ι Per	0 97	0 98	0 95
χ^1 Ori	1 22	1 26	1 21
ξ Peg	0 84	0 85	0 83

Case II.—assume that the two lines are physically separate but are blended extrinsically (by macroturbulence or low resolution) so that the total equivalent width W is the sum of W_1 and W_2, where one line has twice the number of effective absorbers as the other, so that the difference in log η_c is 0.30. Therefore, one has to enter the curve of growth separately for each line to find that point where two lines of this horizontal spacing will add to the observed W.

Case III is similar to Case I, but follows Abt's (1952) approach to the problem of hyperfine structure in solar lines, where the Doppler width is computed from a velocity

$$v^2 = \frac{2kT}{A m_0} + \xi^2{}_{\rm turb} + \left(\frac{c}{\lambda} \cdot \frac{\Delta\lambda}{2}\right)^2 , \tag{14}$$

where $\Delta\lambda$ in the last term is the splitting of the Li doublet (0.152 A), and the $\frac{1}{2}$ factor is empirical.

All three approaches were carried out for the first nine stars to be analyzed, but it was discovered that for Li lines of these strengths the three cases gave essentially the same results for [Li/Ca]; the actual numbers are shown in Table 3. Accordingly, the results quoted hereafter are all Case I values, and the details of the method are described only for Case I.

If the Doppler velocity is composed of a thermal plus a microturbulent component (eq. [14] with the last term omitted), then the latter can be obtained from

$$\xi^2_{\rm turb} = v_{\rm Fe}{}^{*2} - \frac{1.501}{\theta_{\rm exc}{}^*}, \tag{15}$$

where

$$\log v_{\rm Fe}{}^* = 5.48 - \Delta \log W^*/\lambda , \tag{16}$$

and the units are km/sec. The Doppler velocities for Li and Ca follow from this value of $\xi_{\rm turb}$ and the appropriate atomic weights A. The observed log W^*/λ for Li I λ 6707 was corrected for the difference in Doppler widths between Li and Fe before entering the Fe I curve of growth. If $b = \lambda\, v/c$, then the effective log W^*/λ for λ 6707 is as measured plus the correction

$$\log \frac{b(\rm Fe)}{b(\rm Li)} = \log \frac{(\lambda v)_{\rm Fe}}{(\lambda v)_{\rm Li}}, \tag{17}$$

where, for Case I, 1.5 v(Li) is to be used in the denominator. The value of log $\eta_c{}^*$(Li I) can then be read from the Fe I curve of growth. Now, if both Li and Ca are preponderantly singly ionized, it can be shown through the definition of η_c and the Saha and Boltzmann equations that

$$\begin{aligned}\frac{\rm Li}{\rm Ca} = \log \eta_c{}^*(\text{Li I}) - \log \eta_c{}^{\odot}(\text{Li I}) - \langle r(\text{Ca I})\rangle + \log \frac{\kappa^*(\rm Li)}{\kappa^*(\rm Ca)} + \log \frac{v^*(\rm Li)}{v^*(\rm Ca)} \\ + \log \frac{u^*(\text{Li II})}{u^*(\text{Ca II})} - [\, I(\text{Li I}) - I(\text{Ca I})\,]\cdot\Delta\theta + \text{constant}\,,\end{aligned} \tag{18}$$

where the r(Ca I) values are obtained as described for Fe II, the I's are the ionization potentials so that the bracket has the value −0.721 eV, and for Case I the constant is +0.15. The equivalent width of λ 6707 in the Sun has been taken as 3.7 mÅ, following Greenstein and Richardson.

It was felt that a full curve-of-growth treatment was unwarranted for the 16-Å/mm spectrograms because of the smaller number of unblended lines, the lower accuracy of the equivalent widths on account of the lower signal/noise ratio, and the practical consideration that plates of some 40 stars were to be analyzed. Accordingly, a "shortcut" procedure was used whereby the Ca I lines in effect served as a scale from which the Li I abundance was read, and from which the value of [Li/Ca] followed after small corrections for differential ionization, etc., with respect to the Sun. The details are as follows.

A plot of the spectroscopically determined values of $\Delta\theta$ as a function of main-sequence spectral type shows that the systematic change of $\Delta\theta$ in the interval F5–G8 is surprisingly small (Fig. 3*a*), and although there is a suggestion of a small slope in the sense expected, a constant value of $\Delta\theta = -0.01$ seems to be a good approximation for this entire range. There is, on the other hand, a clear variation of $[v_{\rm Fe}] = \log (v_{\rm Fe}{}^*)/(v_{\rm Fe}{}^{\odot})$ over the same interval (Fig. 3*b*). If, as before, the total $v_{\rm Fe}{}^*$ is separated into a turbulent component and a mass-dependent term, $v_{\rm Ca}{}^*$ and $v_{\rm Li}{}^*$ can be calculated. The procedure is then to plot a Ca I curve of growth of log W^*/λ versus log $\eta_{c\odot} + 0.01\,\epsilon$. The empirical solar curve is then fitted to these points, and entered with

$$\log \frac{W^*}{\lambda} + \log \frac{b_{\rm Ca}}{b_{\rm Li}}$$

for the λ 6707 line, where the second term depends only upon spectral type. This value of log $\eta_c{}^*$(Li I) is then corrected by

$$-\langle r(\text{Ca I})\rangle + \log \frac{v_{\rm Li}{}^*}{v_{\rm Ca}{}^*} + 0.88\,,$$

where the final constant contains the differential terms involving absorption coefficients, partition functions, and solar parameters; the second term depends only upon spectral type. The result is [Li/Ca]. The weight *b* is attached to this type of determination. The method seems to do adequate justice to material of this quality. A plot of the 4-Å/mm [Li/Ca] values (of weight *a*) against the 16-Å/mm results for the seven stars for which both are available suggests that there is a small systematic difference between the two, amounting to about 0.1 in the logarithm. The 16-A/mm values of [Li/Ca] in the eleventh column of Table 2 are as directly determined, but the "adopted [Li/Ca]" values of the fourteenth column have been corrected by −0.10 to reduce them to the 4-Å/mm system.

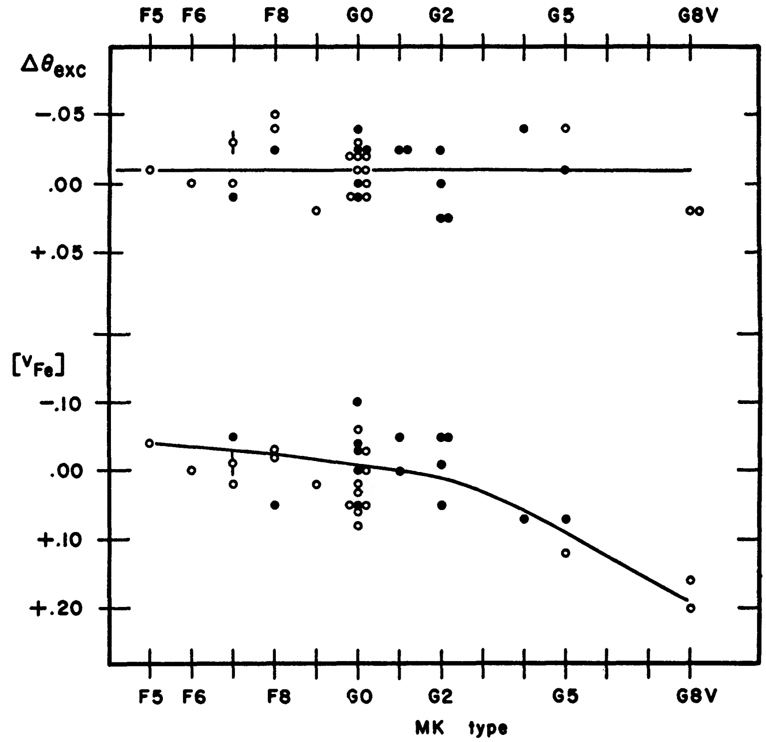

FIG. 3.—*Upper half:* $\Delta\theta_{exc}$ versus main-sequence MK types for stars analyzed by Wallerstein (1962; here *filled circles*) and by Herbig (this paper; *open circles*). The horizontal line at $\Delta\theta_{exc} = -0.01$ corresponds to the mean value adopted for this spectral interval in the "shortcut" method, Sec. II. *Lower half:* the variation of [v_{Fe}] with main sequence spectral type; the coding is as in upper half. The solid line shows the mean relation adopted for use in the "shortcut" method.

There remained spectrograms of some forty-eight stars for which curves of growth were not constructed, in most cases because the plates were not of spectrophotometric quality on account of streaks, underexposure, or other defects. In an effort to salvage as much of this material as possible, since it was impractical with the limited amount of telescope time available to repeat all the spectrograms, a graduated system of eye estimates of the intensity of Li I λ 6707 was set up, using as a scale the strengths of nearby Fe I and Ca I lines in the same spectrum. Thus, $I = 3$ denoted a line equal in strength to Fe I λ 6703, and $I = 7$, one equal to Ca I λ 6717. These eye estimates were made for all the 16-Å/mm plates, and to a first approximation, should be independent of line-broadening and metal-abundance differences. There is an acceptable degree of correlation between the I numbers (given in the thirteenth column of Table 2) and the measured values of [Li/Ca]; the two are plotted against each other in Figure 4. The weight *c* [Li/Ca]'s in the fourteenth column of Table 2 are simply read, with I as argument, from the smooth curve of Figure 4. These c-weight results are statistically useful, but one should not take them too literally in individual cases, since the horizontal scatter in Figure 4 shows that errors of ± 0.2 in [Li/Ca] are to be expected.

All the individual values of [Li/Ca] have been combined in the "adopted [Li/Ca]" values of column (14) of Table 2, where 4-Å/mm determinations have been given weights of 4, 16-Å/mm determinations weight 2, and results from eye estimates weight 1. The total weight is reflected in the letters a, b, c of column (16). It is unfortunate that, on account of the magnitude of the observational program, there rarely was opportunity to obtain more than one spectrogram per star so that the accuracy of the analyses is correspondingly lower than is usual for work at these dispersions. This is not too serious a matter in a survey program of this kind, but it should not be forgotten by those who might plan to use the atmospheric parameters of Table 2 for some other purpose.

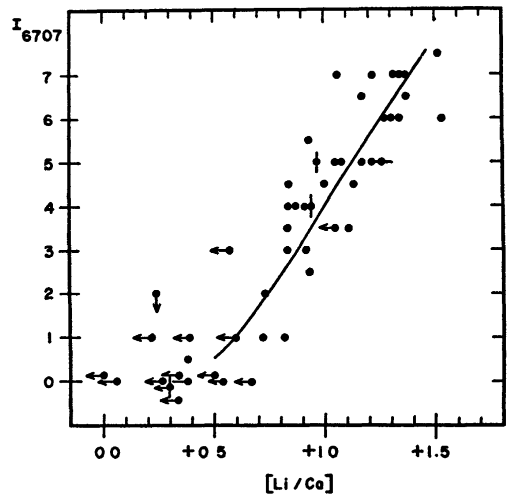

FIG. 4.—The relationship between eye estimates of λ 6707 strength on the 16-Å/mm plates (= I_{6707}) and the corrected 16-Å/mm values of [Li/Ca]. Arrows indicate upper limits, and bars uncertain values. Values of [Li/Ca] read from the solid line are given c weight.

III. LITHIUM ABUNDANCES IN CLUSTERS OF KNOWN AGE

The most direct means of evaluating the variation of Li abundance with time is through the F- and G-type dwarfs in star clusters whose ages can be inferred from H-burning considerations. Although this part of the program has not been carried as far as is possible, further data will accumulate slowly on account of the long photographic exposures required. Information is now available on the Hyades, Pleiades, and Coma clusters and on a number of T Tauri stars, the latter mostly through the observations of Bonsack and Greenstein. It should be possible eventually to add some stars in the α Persei cluster and the Orion Sword clustering to this list. The detailed results are as follows.

Hyades.—As part of this program, 16-Å/mm spectrograms were obtained of the seven F- and G-type main-sequence stars listed in Table 4 which, according to Van Bueren (1952), are physical members of the Hyades cluster. The last star (VB 120) may or may not belong to the cluster, as noted in Table 4, but if it is a member, it is far enough above the main sequence to eliminate it from the present consideration of dwarfs alone. Five of these seven stars have also been measured for [Li/Ca] by Wallerstein, Herbig, and Conti (1965); their results are given in the last column of Table 4. The spectrograms used in the two investigations were the same, but the microphotometers and personnel were different, and the methods of analysis were not entirely identical, although both were differential comparisons with the Sun through Ca I. Comparison of the last two columns of Table 4 shows no obvious difference between the two systems, although the large Δ[Li/Ca] = 0.6 for VB 19 is disturbing.

Pleiades.—Only one Pleiades member was observed, the G0 V star H II 996. The (corrected) value of [Li/Ca] is +1.9, which must be given a weight between *b* and *c* on account of the lower dispersion used (32 Å/mm).

TABLE 4

LITHIUM ABUNDANCES OF HYADES CLUSTER MEMBERS

Van Bueren No	HD	Mount Wilson Spectral Type	Corrected [Li/Ca]*	[Li/Ca] (Wallerstein *et al*)
2	20439	G1	+1 7†	+1 7
19.	26784	F7	+1 3	+1 9
23‡	27149	G4	≤+1 1	+1 2
50§	27836	G1	+1 1	+1 3
58	27989	G4	+1 2	+0 9
75	28363	F8	+1 4	
120‖	30712	G5	≤+0 8	

* These [Li/Ca] values are weight-*b* determinations, and have been corrected by −0 10 to adjust to the 4-Å/mm abundance system; see Sec II

† Mean of two spectrograms, reduced separately; the individual values were +1 7, +1 8

‡ Double-line spectroscopic binary. The analysis listed here is of the shortward set of lines on 1963 Jan 16, 2^h45^m U T Because of the line doubling, the [Li/Ca] value is of lower weight than the others

§ The H, K emission was discovered by Joy and Wilson (1949)

‖ VB 120 was regarded as a cluster member by both Van Bueren and R E Wilson, on the basis of its motion, but it was not accepted as such by Johnson, Mitchell, and Iriarte (1962) apparently because of its displacement from the cluster main sequence The [Li/Ca] value is much lower than those of all the other Hyades members observed The emission in H and K lines was discovered by Joy and Wilson (1949)

TABLE 5

LITHIUM ABUNDANCES OF COMA CLUSTER MEMBERS

Trumpler No	MK Spectral Type (Mendoza 1963)	Corrected [Li/Ca]
53	F9 V	+1 6
58	F9 V	≤+0 9
162	F7 V	+1 1

Coma.—The three Coma members listed in Table 5 were also observed at 32 Å/mm. All have rather weak lines, which made the analysis difficult.

In Figure 5 are plotted (on the left side) the [Li/Ca] values for these cluster stars against the logarithms of their H-burning ages (Henyey, LeLevier, and Levée 1959). The Bonsack and Greenstein (1960) [Li/metal] values for 5 T Tauri stars, together with Herbig's (1964*b*) [Li/Ca] value for FU Ori,[1] are all plotted arbitrarily at $t = 10^6$ years, while the Sun is shown at $t_\odot = 4.7 \times 10^9$ years.

The general progression of points in Figure 5 supports the hypothesis of a general decline in [Li/Ca] with age. It must be remembered, however, that since the spectral

[1] The analysis of the F spectrum of FU Ori gave [Li/Ca] = +1.9; since the method differed slightly from that used here (Sec. II), the systematic correction of Δ[Li/Ca] = −0.1 was not applied.

types of the normal stars plotted in Figure 5 range between F7 and G4, there may well be a substantial spread in both t_c and $L(0)$ over this interval so that even given perfect data, a real fuzziness in such a plot may be anticipated. The exponential curve for $L(t)/L(t_\odot)$, obtained from equation (7) with $t_c = 1.32 \times 10^9$ years and $L(0)/L(t_\odot) = 35$ is also shown in Figure 5, where now the scale on the right margin is to be used. A critical comparison of the observations with the curve is hardly possible, but there is no striking discrepancy except that the T Tauri stars in the mean have about three times more Li than the curve predicts; we return to this matter in Section VII.

It is obvious that more observational data are needed, particularly for clusters younger than 10^8 years and older than 10^9 years. The first gap can be filled, as already mentioned, but the other will be much more difficult since even the most favorable clusters are quite

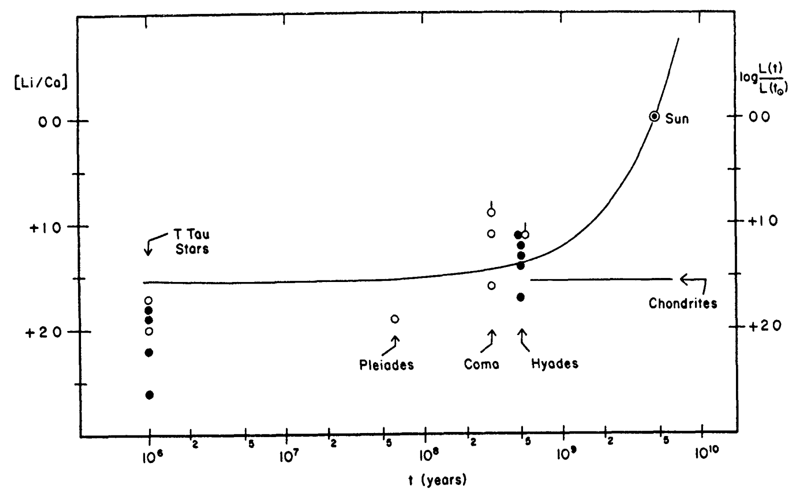

FIG 5.—The dependence of [Li/Ca] (*left margin*) on age for T Tauri stars (arbitrarily plotted at $t = 10^6$ years), 1 G dwarf in the Pleiades, 3 F dwarfs in Coma, 6 in the Hyades, and the Sun, which is shown at $t = 4.7 \times 10^9$ years Filled circles are 16-Å/mm results, while open circles correspond to 32-Å/mm results or less certain values The scale of log $L(t)/L(t_\odot)$ on the right corresponds to the exponential curve, which has $t_c\odot = 1\ 32 \times 10^9$ years, and represents the rate of Li depletion predicted by the elementary theory with $A = 0$ (see Sec I) The horizontal asymptote to the exponential is given by the chondritic lithium abundance, as shown by the line on the right. The star clusters are plotted according to their H-burning ages after Henyey, LeLevier, and Levée (1959). The exponential curve is determined solely by the solar and meteoritic data; the stellar data are completely independent of it.

distant. Thus, main-sequence G0 stars in NGC 752 ($t = 10^9$ years) are expected at about $m_v = 12.5$, in M67 ($t = 10^{10}$ years) at $m_v = 14$, and in NGC 188 ($t = 1.5 \times 10^{10}$ years) at about $m_v = 15.5$. Only NGC 752 seems attainable at adequate dispersion by conventional techniques, and even there (since more than one star should be observed) a major effort will be required.

A few stars that have been assigned by Eggen (1960*a*, *b*) to the Sirius or Hyades moving groups occur in Table 2; I am indebted to Dr. Eggen for providing me with up-to-date lists of stars that he considers to be group members on the basis of recent data. These stars and their [Li/Ca] values are listed in Table 6. The number of stars is far too small for any conclusions to be drawn, but the similarity of the [Li/Ca] values for the four Sirius-group stars is encouraging.

IV. CORRELATION OF LITHIUM ABUNDANCE WITH OTHER PROPERTIES

If the present Li abundance of an F- or G-type dwarf is indeed the result of convective destruction of Li on a long time scale, then there should be some correlation with other properties of the stars. One might expect in particular that the statistics of Li abundance should reflect the deepening of the surface convection zone as one goes from type F to the K dwarfs (i.e., a shortening of t_c in eq. [7]) and possibly also the greater effectiveness of Li-burning during contraction —i.e., a decrease in L(0)—as one goes down the main sequence in the same direction.

Table 7 gives the number of stars in each of four Li-abundance groups as a function of main-sequence spectral type. The data are for eighty-four stars, all from Table 2; stars more distant than 20 pc or having particularly uncertain [Li/Ca] values were excluded. It is seen that there is a striking dependence of the shape of the Li frequency function upon spectral type: at types later than about G2, there is a conspicuous lack of Li-rich dwarfs, ξ Boo A at G8 V and l = 25 being the notable exception. The complete absence

TABLE 6

MOVING GROUP STARS FOR WHICH [Li/Ca] VALUES ARE AVAILABLE

Star	Spectral Type	Corrected [Li/Ca]	Weight
	a) Hyades Group		
9 Cet. .	dG2	+1 2	*b*
HD 4747	dG7	≤+0 5	*c*
18 Pup	dF7	+1 1:	*c*
	b) Sirius Group		
HD 11131	dG1	+1 0	*b*
χ^1 Ori	G0 V	+1 26	*a*
η CrB .	G2 V	+1 2	*b*
HR 7451	F8 V	+1 2	*b*

TABLE 7

THE DEPENDENCE OF LITHIUM ABUNDANCE ON SPECTRAL TYPE (LUMINOSITY CLASS V ONLY)

SPECTRAL TYPE	l≡ANTILOG [Li/Ca]				FRACTION WITH l≥5
	>20	20–10	10–5	<5	
F5, F6, V*	1	2	.	1	0 75
F7*	.	3	2	1	83
F8, F9	2	1	1	2	67
G0	1	6	2	6	60
G1	1	1	4	2	75
G2 .	3	1	1	8	38
G3, G4			2	6	25
G5, G6			5	6	45
G7, G8	1			12	08
≥K0 V					(0 00)

* Selectivity was exercised in types F5–F7 in that stars having rotationally broadened lines ($v \sin i \geq 20$ km/sec) were rejected

of detectable Li I in the K, M, and Me dwarfs (although no analyses are available except of three K dwarfs by Bonsack 1959) is also to be noted. At the other end of the table, Li-poor F5–F7 stars are definitely in a minority. The results are qualitatively in accord with expectation, but in the absence of some theoretical guidance one cannot say more.

Some correlation might also be expected between Li abundance and kinematic characteristics. To investigate the dependence of [Li/Ca] upon space motion, those stars in Table 2 within 20 pc were divided into three groups of diminishing Li abundance,

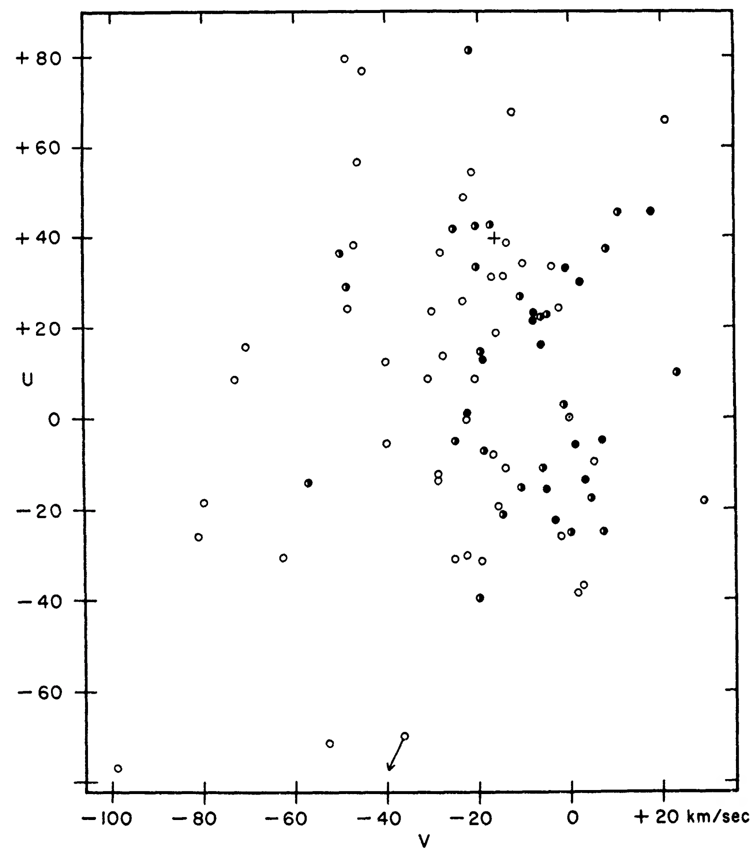

FIG. 6.—The distribution of F5–G8 dwarfs within three lithium-abundance classes over the UV velocity plane. *Filled circles:* stars with $l > 15$; *half-filled circles:* stars with $15 > l > 5$; *open circles,* stars with $l < 5$. The Sun is at the origin, and the Hyades is represented by the cross near (+40, −16) km/sec. The generally low Li content of the high-velocity stars is apparent, as is the preference of Li-rich stars for the lower velocities. Positive U is in the direction away from the galactic center, and positive V is in the direction of galactic rotation.

having $l(\equiv$ antilog [Li/Ca]$) > 15$, 5–15, and <5. The space velocity vectors (U, V, W) for these stars were taken from the compilation by Eggen (1962) or, in a few cases, from that by Gliese (1957). A plot of the UV values for these three groups is shown in Figure 6, where it is apparent that the Li-rich group tends to have small to moderate velocities in the UV plane while many Li-poor stars have high velocities. The lack of stars with high Li content among the high-velocity population is especially noteworthy.

A quantitative measure of this correlation can be obtained by computing the velocity dispersions along the axes of the velocity ellipsoids of the three groups. It was assumed that all the ellipsoids had the same centers and orientations: the long axes (σ_1) directed to $l^{II} = 20°$, $b^{II} = 0°$; second axes (σ_2) to $l^{II} = 110°$, $b^{II} = 0°$; and third axes (σ_3) to $b^{II} = 90°$. Furthermore, it was assumed that all their centers were located by the "basic solar motion" (Dyer 1956). This latter assumption is an increasingly poor one for the high-velocity stars, but the error should not be serious for the present demonstration. The resulting dispersions are given in Table 8. The increase in σ_1 and σ_2 with decreasing l is apparent, but σ_3 (in the direction perpendicular to the galactic plane) shows no change.

There is no conflict with expectation in these results, but again the correspondence has to remain qualitative until theoretical t_c and $L(0)$ values for stars of this mass range become available. Or, in different words, in assessing these results it must not be forgotten that a given l value may indicate a very old F8 star but a very young G8 dwarf.

It might be anticipated that there should also be a correlation between the Li and metal abundances of stars of a given mass. This would be so only if there exists a tight relationship between metal abundance and age. If other factors can enter into the metal abundance, then any correlation with Li will be masked, since we are concerned here with stars whose metal abundances are expected to differ only by small amounts from those of the Sun or the Hyades.

The metal abundances of the stars in Table 2 are best obtained not spectroscopically (since spectroscopic determinations of [Fe/H] are subject to some individual uncertainty) but rather by narrow-band photometry. Strömgren's m_1 index is available for many of the stars in Table 2 (Strömgren and Perry 1964; I am much indebted to Dr. Strömgren

TABLE 8

VELOCITY DISPERSIONS (IN KM/SEC) FOR NEARBY STARS OF HIGH, MEDIUM, AND LOW LITHIUM ABUNDANCES

l	No of Stars	σ_1	σ_2	σ_3
>15	13	19 0	14 4	19 2
5–15	27	29 6	19 5	22 9
<5	44	46 4	48 5	19 2

for a prepublication copy of that catalogue), and for the present purpose has been converted to Δm_1, a measure of the difference in metal content between the star in question and that of the Hyades (Strömgren 1963). However, it is more instructive to plot [Fe/H] against [Li/H], rather than against [Li/Ca], because of the probable correlation of Ca and Fe abundances. Therefore, in Figure 7 is shown [Fe/H] versus

$$[\mathrm{Li/Ca}] + [\mathrm{Fe/H}] = [\mathrm{Li/H}] + \text{constant}\,,$$

where the "constant" is [Fe/Ca]. The open circles in Figure 7 represent G1–G8 dwarfs, the filled circles F5–G0 stars. The vacant region in the lower left-hand part of the figure is due to the detectability limit on Li I λ 6707. That region is presumably populated by some of the stars for which only upper limits on [Li/H] are available.

The envelope of G star points in Figure 7 shows a tendency to obey expectation, in that the Li-rich G dwarfs are those with the higher metal abundances, and that there are certainly no low-metal G dwarfs in the sample with l values as high as 4. The F stars, on the other hand, show no tendency toward lower metal abundances at the lower Li values. The point at (+1.04, −0.44) represents χ Her, F9 V, for which the metal deficiency has been confirmed spectroscopically (see Table 2). The same star is also a conspicuously aberrant point in velocity space; it is the high-Li point at (+46, +18 km/sec) in Figure 6.

There is another complication that will ultimately have to be considered in evaluating the distribution of points in Figure 7. This is the possible dependence of $L(0)$ upon chemical composition, because Hayashi and Nakano (1963) have shown that the degree of Li depletion during pre-main-sequence contraction depends upon both the helium and metal content.

V. CORRELATION OF LITHIUM ABUNDANCE WITH STRENGTH OF CA II EMISSION

It was noticed very early in the program, as spectrograms accumulated, that there was a tendency for many of the stars having a strong Li line also to have unusually intense emission cores in the H and K-lines of Ca II. The evolutionary interpretation of the decay of Li abundance with time implies such a correlation, because the T Tauri stars possess both strong Li absorption and intense Ca II emission, and the older main-sequence stars show little of either. This does not mean that the two should necessarily decay on the same time scale, since the degree of activity at the chromospheric level (responsible for the Ca II emission cores) may well involve other factors than affect the Li depletion.

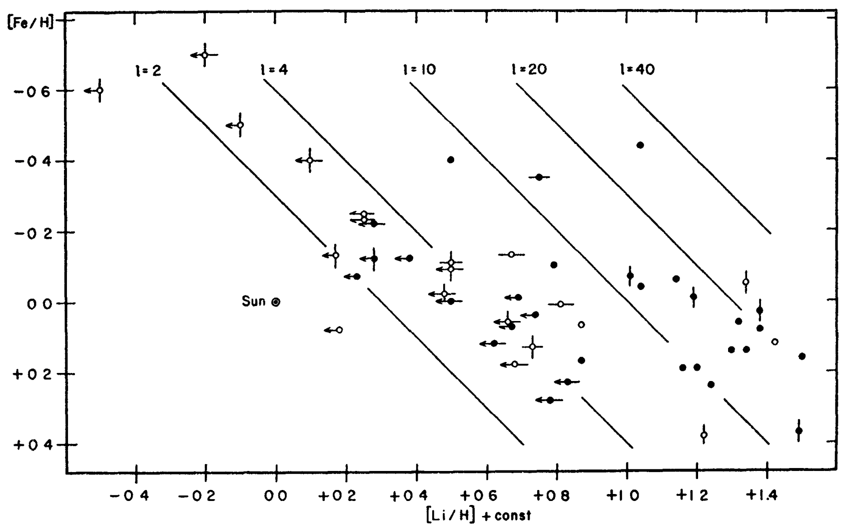

FIG 7.—The dependence of photometric [Fe/H] upon [Li/H]; the sloping lines represent lines of equal *l*. The filled circles denote F5–G0, the open circles G1–G8 dwarfs Horizontal bars indicate data of weight *c*, vertical bars correspond to spectroscopic rather than photometric [Fe/H] values Points with arrows are upper limits The F stars show no apparent dependence of Li upon metal abundance, but the G stars seem to show some correlation.

Due to lack of telescope time, however, it was possible to obtain 16-A/mm spectrograms properly exposed at the centers of H and K for only a limited number of stars, and so the correlation has not been explored as far as would be desirable. Fortunately, Wilson (1962, 1963*b;* Wilson and Bappu 1957) has published lists of estimated intensities of the Ca II emission cores in a number of bright stars. The emission strengths in the stars observed only at Lick have been estimated on Wilson's scale, by intercomparison on a Hartmann spectrocomparator with standards chosen from his lists. The emphasis has been on stars of types G5 and earlier so as to improve the chance of a meaningful correlation, since the incidence of Ca II emission increases sharply to later spectral types. The results are given in Table 2, and are plotted against [Li/Ca] in Figure 8.

The sloping band of points inclosed by the lines in Figure 8 includes all the positive observations (except that for ξ UMa B, discussed in Sec. VI). The following conclusions can be drawn from Figure 8: (1) There is a definite tendency in this sample of G0–G5 dwarfs for the strongest Ca II emission to appear in stars of rather high Li abundance, but the total spread in [Li/Ca] is large, perhaps as much as 0.7 in the logarithm at a given emission strength; (2) at intermediate values of [Li/Ca], stars are found with all values of Ca II emission intensity; but (3) at both low and very high values of [Li/Ca], only stars with low and very high Ca II emission intensities, respectively, have been observed.

It is concluded that there is a definite *statistical* correlation of emission strength with [Li/Ca], as expected on the evolutionary picture, but the relationship is not a tight one and cannot be trusted in individual cases. However, it is important that the Ca II emission intensities be placed on a better quantitative footing. As far as internal accuracy is concerned, carefully made eye estimates are quite competitive with microphotometer tracings for features of this kind, but for the present purpose, it is very desirable to have the intensities on a photometrically calibrated system. It seems more important, as a next step, to straighten out this matter of calibration than simply to extend the present system to more stars.

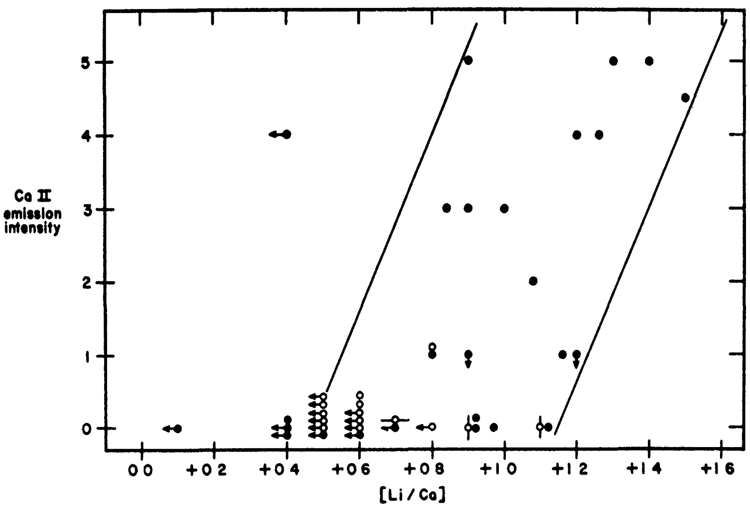

FIG. 8.—The relationship between the intensity of H-K emission (on Wilson's scale) and [Li/Ca] for F5–G5 dwarfs Filled circles correspond to weight *a* and *b* [Li/Ca]'s, while open circles are of weight *c*. Arrows indicate upper limits, and bars uncertain values. The point in the upper left is ξ UMa B, discussed in the text. (*Note added in proof:* Since this paper was written, new observations have shown that 58 Eri, plotted at (+0.9, 5) in this figure, has [at least at the present time] an H-K emission intensity nearer a value of 3 than 5. If the point for 58 Eri is moved downward in the figure by that amount, the dispersion of points is appreciably reduced.)

VI. BINARY STARS

Since the components of a binary star must be effectively of the same age, their Li abundances should be accordant when mass differences are taken into account. No particular effort has been made in this program to concentrate on binaries, either visual or spectroscopic, but a few pairs have been observed incidentally.

Perhaps the most interesting cases are ξ Boo (G8 V + dK5) and λ Lep (F6 V + K2 V). In both pairs, the primaries are Li-rich ([Li/Ca] = +1.39 and +1.08, respectively), while the Li I λ 6707 line is undetectable in the secondaries at 16 Å/mm. In ξ Boo, this was noted also by Wilson (1963*a*). These are clear examples in pairs of stars having the same age but different masses, of the phenomenon shown in Table 7, where there is a conspicuous lack of stars with detectable Li I λ 6707 later than type G8. On the other hand, if the stars are not so late in type, both components behave very similarly. Both stars of the binary 53 Aqr (dG1 + dG2) have very large [Li/Ca] values. The short-period visual binary (P = 5.7 years) δ Equ (F8 V) was observed at 4 Å/mm as one star, but the radial velocity difference at the time of observation was sufficient to separate the two spectra. Both stars have λ 6707 present, and in about the same intensity ratio as other lines in the neighborhood. Similarly, the two components of the binary η CrB (G2 V) have been observed separately (as well as together, the latter result being given in Table 2); their λ 6707 lines are of very similar strength.

Spectrograms are available also for two spectroscopic binaries: δ Tri ($P = 9.9$ days) and ι Peg ($P = 10.2$ days), although known formerly as single-line systems, show the spectra of the secondaries in the red at 4 Å/mm. In both cases, the relative strength of λ 6707 is very similar in the two components.

In fact, the behavior of these double stars conforms so well to expectation that the anomalous behavior of the two components of ξ UMa is striking. This visual pair has a period of 59.8 years; both types are G0 V. Component A, slightly the brighter ($\Delta m = 0.4$ mag.) is a single-line spectroscopic binary with $P = 669$ days, a high Li abundance ([Li/Ca] $= +1.20$), but with weak Ca II emission cores. B is also a single-line binary but of much shorter period, $P = 3.98$ days; it has no detectable λ 6707 at 4 Å/mm ([Li/Ca] $\leq +0.4$), but does have quite strong Ca II emission cores. The combination of high Li and weak emission in A is not unprecedented (see Fig. 8), but the low Li and strong Ca II emission of B is conspicuously discrepant in Figure 8. Since B is the binary of shortest period observed in this program, one might speculate that synchronous axial rotation might be able to force a slow circulation that would have the effect of destroying surface Li more rapidly than in a non-rotating G0 dwarf, while A convects at the normal

TABLE 9

RELATIVE RATES OF STAR FORMATION AS DERIVED FROM LITHIUM STATISTICS

Present Value of l	Corresponding Age, τ (unit $= 10^9$ years)	No of G1–G4 Stars in l Interval	$n(\Delta l)/\Delta\tau$	No of G0–G2 Stars in l Interval	$n(\Delta l)/\Delta\tau$	No of G3–G5 Stars in l Interval	$n(\Delta l)/\Delta\tau$
35	0						
		4	5 4	5	6 8	0	0
20	0 74						
		2	2 2	8	8 7	0	0
10	1 66						
		7	7 6	7	7 6	6	6 5
5	2 58						
		16	1 3	16	1 3	9	0 7
0:	15						

rate. But this would explain only the difference in Li content between A and B; it is not obvious that the weak Ca II emission in A and the strong emission in B can be accounted for in the same manner. The system ξ UMa may constitute a real exception to the general rules of the Li phenomenon, and deserves continued attention.

VII. EVOLUTIONARY IMPLICATIONS; SUMMARY AND CONCLUSIONS

There is considerable opinion to the effect that in the Galaxy star formation in the past was at least as active as it is today. If true, and if the F- and G-type dwarfs within 20 pc are a fair sample of such stars of all ages in proportion to their true frequencies in this part of the Galaxy, then the statistics of Li abundance should reflect that fact, if indeed Li can be used as an age indicator. As already shown, in the Sun the time constant for exponential Li decay is 1.32×10^9 years, and the times τ required for the solar Li abundance to be reduced successively to $l = 20, 10, \ldots$, etc., from an initial value of $l = 35$ can be obtained from equation (7). These times, measured backward from the present, are given in the second column of Table 9; in the notation of Section II, $\tau = t_\odot - t$. The number of stars observed in each Δl range, $n(\Delta l)$, can be found in Table 7. The numbers for the G1–G4 interval appear in the third column of Table 9. Now, if one assumes that the average G1–G4 star will leave the main sequence after 15×10^9 years, then $n(\Delta l)/\Delta\tau$ should be proportional to the number of stars formed per unit time about $\tau + \Delta\tau/2$ years ago, where $\Delta\tau$ represents the time required to deplete l by Δl. The interval G1–G4 is approximately centered on the Sun, but the data in Table 7 have already shown that there is an important change in the character of the Li statistics near G2. Therefore, Table 9 also lists $n(\Delta l)/\Delta\tau$ values for the spectral intervals G0–G2 and G3–G5, always with a main-sequence lifetime of 15×10^9 years.

These "relative rates of star formation" in Table 9 all show the same property, namely, that there are *too few Li-poor G dwarfs* in the solar vicinity to support the assumptions of the preceding paragraph. If the hypothesis is to be maintained, then either (*a*) there must be a means by which some of these stars replenish their surface Li supply; or (*b*) the sample of G dwarfs in the solar neighborhood is relatively poor in stars older than about 2 or 3×10^9 years; or (*c*) in respect to its Li abundance, the Sun is not a representative G2 dwarf.

If there is some process (such as nucleosynthesis or accretion) by which G dwarfs are able to replace their surface Li, then the exponential curve in Figure 5 will level off and at large values of t, go to the limit given by equation (6). In the present state of knowledge, little can be said about this possibility.

It has already been noted that the exponential of Figure 5 does not pass through the T Tauri star points; or, in different words, that the Li/Si ratio in the chondritic meteorites is only about one-third of that in the T Tauri stars. It is true that the asymptote to the exponential curve at [Li/Ca] $\approx +1.5$ (which comes directly from the solar and meteoritic data) is the same as the upper limit found spectroscopically for F and G dwarfs in the general field. But it has not been proved that the [Li/Ca] values in this paper as a *system* are compatible with that of the Bonsack-Greenstein results for T Tauri stars. In this regard, an independent study of the [Li/Ca] values in some of these same F and G dwarfs by Mr. Richard Wolff, using the same method as in Section II but with an independently determined set of log $\eta_{c\odot}$'s, suggests that the [Li/Ca] values of weight *a* in Table 2 may be somewhat too small. Furthermore, the meteoritic:solar Li value of 35 used here certainly will be modified as experimental data improve. For all these reasons, I recommend that judgment be suspended for the moment on the question whether the T Tauri stars do or do not have more Li than the exponential theory predicts.

In summary, the hypothesis that the variation of Li abundance in F5–G8 dwarfs may be due to slow convective depletion is supported by the following observational results:

1. The Li contents of those F and G dwarfs that have been observed in clusters of known age conform reasonably well to prediction from solar and meteoritic data (Sec. III).
2. The observed correlation of [Li/Ca] with space velocity is qualitatively in the correct sense, while the correlation of [Li/Ca] with metal abundance is in the expected direction for G dwarfs, but not for F's (Sec. IV).
3. The frequency function of [Li/Ca] varies with spectral type in the expected sense (Sec. IV).
4. There is a statistical dependence of Li content upon Ca II emission intensity as predicted, but there is also a large scatter which requires explanation. However, a quantitative calibration of the emission intensities is very desirable (Sec. V).
5. In general, both members of binary systems have accordant Li abundances when mass differences are taken into account.

On the other hand, the hypothesis cannot by itself explain:

6 The existence of a star like χ Her, with rather high space motion and low metal content (about 0.4 times the solar value), yet with a Li/H value about 12 times solar. The explanation may be that small variations in metal content cannot be taken literally as age indicators in such stars.

7. The existence of a star like ξ UMa B, with a low Li abundance, while its companion has a high Li content. The explanation may lie in the fact that B is a short-period spectroscopic binary, and hence may be better mixed than A.

8. The excess of nearby stars with high Li contents, contrary to evolutionary expectation if the sample is a fair one.

In conclusion, the hypothesis is quite successful in explaining a number of observational facts that would otherwise be rather puzzling and, if it can be buttressed with some subsidiary premises, may well be able to cope with objections such as those above. But it is often that initial explanations do not survive; there are more observational checks to be applied, and it seems safe to predict that the idea may well be tested critically in the next few years.

It is a pleasure to acknowledge the indefatigable energy and skill devoted by Mr. K. Wilde to the microphotometry of the spectrograms used in this investigation. I also thank Drs G. W. Preston and R. Weymann for instructive discussions on various aspects of the problem. Some of the reductions were performed on the Observatory's IBM 1620 computer, for which the National Science Foundation provides partial support.

REFERENCES

Abt, A. 1952, *Ap J.*, **115**, 199.
Allen, C. W. 1963, *Astrophysical Quantities* (2d ed ; London: Athlone Press), p. 95
Aller, L. H 1953, *Astrophysics: The Atmospheres of the Sun and Stars* (1st ed ; New York: Ronald Press Co), p. 292.
——— 1963, *Astrophysics: The Atmospheres of the Sun and Stars* (2d ed.; New York: Ronald Press Co.), p. 382.
Aller, L. H., and Greenstein, J. L 1960, *Ap. J. Suppl* , **5**, 139.
Böhm, K 1963, *Ap. J.*, **138**, 297.
Bonsack, W K 1959, *Ap. J* , **130**, 843.
Bonsack, W K , and Greenstein, J. L 1960, *Ap J* , **131**, 83.
Claas, W J. 1951, *Rech. Astr Obs. Utrecht*, Vol **12**, pt 1
Dyer, E. R. 1956, *A.J* , **61**, 228
Eggen, O. J. 1960*a*, *M.N.*, **120**, 540
———. 1960*b*, *ibid* , p. 563.
———. 1962, *Roy. Obs Bull* , No 51.
———. 1963, *A J.*, **68**, 496
Ezer, D., and Cameron, A G. W. 1963, *Icarus*, **1**, 422
Gliese, W 1957, *Mitt Astr Rech.-Inst Heidelberg*, Ser A, No 8
Goldberg, L., Müller, E , and Aller, L H. 1960, *Ap J. Suppl* , **5**, 1.
Greenstein, J. L., and Richardson, R 1951, *Ap J* , **113**, 536
Hayashi, C , and Nakano, T 1963, *Prog Theor Phys* , **30**, 460
Henyey, L. G , LeLevier, R , and Levée, R. D. 1959, *Ap J* , **129**, 2
Herbig, G H. 1964*a*, *Ap J* , **140**, 702
———. 1964*b*, paper to appear in the proceedings of the Flagstaff symposium on the Hertzsprung-Russell Diagram, June 1964.
Johnson, H L , Mitchell, R. I , and Iriarte, B 1962, *Ap J.*, **136**, 75.
Joy, A. H , and Wilson, R. E. 1949, *Ap J.*, **109**, 231.
Kuhi, L. V. 1964, *Ap J* , **140**, 1409.
Mendoza V., E. E. 1963, *Bol Obs. Tonantzintla y Tacubaya*, **3**, 137.
Mutschlecner, P. 1963, *A J.*, **68**, 287.
Roman, N G 1955, *Ap. J Suppl* , **2**, 195.
Shima, M , and Honda, M. 1963, *J. Geophys Res.*, **68**, 2849
Strömgren, B. 1963, *Basic Astronomical Data*, ed K. A Strand (Chicago: University of Chicago Press), chap ix.
Strömgren, B., and Perry, C. (in preparation).
Suess, H. E., and Urey, H. C. 1958, *Hdb. d. Phys* , **51**, 296
Van Bueren, H 1952, *B A.N.*, **11**, 385.
Wallerstein, G. 1962, *Ap J. Suppl.*, **6**, 407
Wallerstein, G., Herbig, G H., and Conti, P. 1965, *Ap J.*, **141**, 610.
Weymann, R., and Moore, E. 1963, *Ap J.*, **137**, 552
Wilson, O. C. 1962, *Ap. J.*, **136**, 793.
———. 1963*a*, *Pub. A.S.P.*, **75**, 62
———. 1963*b*, *Ap J.*, **138**, 832.
Wilson, O C., and Bappu, M K V. 1957, *Ap J.*, **125**, 661.
Wrubel, M 1949, *Ap. J.*, **109**, 66.